Normal-state transport properties of $YBa_2Cu_3O_{7-y}/PrBa_2Cu_3O_{7-y}$ superlattices

L. M. Wang and H. C. Yang
Department of Physics, National Taiwan University, Taipei 10764, Taiwan, Republic of China

H. E. Horng
Department of Physics, National Taiwan Normal University, Taipei 11718, Taiwan, Republic of China
(Received 27 November 1995; revised manuscript received 13 December 1996)

This work measures the resistivity and Hall coefficient R_H for a series of $YBa_2Cu_3O_{7-y}/PrBa_2Cu_3O_{7-y}$ (YBCO/PBCO) superlattices. The Hall coefficient R_H systematically varies with different thicknesses of YBCO or PBCO layers. The Hall number decreases with a decreasing thickness of YBCO layers or increasing thickness of PBCO layers. We investigate the temperature dependence of the Hall angle in YBCO/PBCO superlattices as well. The cotangent Hall angle is also observed to follow a universal T^2 dependence in all superlattices, i.e., $\cot\theta_H=\alpha T^2+C$ where both α and C change with the layer thickness. From the results presented herein, we believe that the reduction in carrier density, caused by the magnetic scattering effects and hole filling which occur near the interface, leads to the depression of T_c in the YBCO/PBCO superlattice. [S0163-1829(97)05034-0]

I. INTRODUCTION

Since superconducting properties of the high-T_c superconductors heavily depend on the layer structure, layer by layer growth of superconducting superlattices is expected to allow us to prepare samples with a new crystal structure which does not otherwise naturally exist. Experimental techniques to prepare epitaxial high-T_c superconducting films have been established and the initial artificial construction of $YBa_2Cu_3O_{7-y}/DyBa_2Cu_3O_{7-y}$ superlattice was reported by Triscone *et al.*[1] Artificially grown superlattices of other types of materials have also attracted a wide interest.[2,3] An interesting structure is a superlattice consisting of superconducting $YBa_2Cu_3O_{7-y}$ (YBCO) and semiconducting $PrBa_2Cu_3O_{7-y}$ (PBCO). Two materials, YBCO and PBCO oxide compounds, are isomorphic and have the advantage of a small lattice mismatch, so that artificial growth of YBCO/PBCO superlattices have attracted great interest. The high quality of epitaxial growth has been confirmed, in addition the YBCO layers remain superconducting down to the thickness of 12 Å.[4,5] As is well known, the critical temperature for YBCO/PBCO superlattices decreases with a decrease in the thickness of individual YBCO layers or an increase in the individual PBCO layers. However, the origin of the T_c depression in the YBCO/PBCO superlattices remains unclear. It is also not known how the variations of the carrier concentration affect the T_c depression. Current investigations are attempting to understand such effects.[6]

On the other hand, Chien *et al.*[7] reported a relationship between Hall $\cot\theta_H$ and T^2, revealing considerable regularities in this phenomenon. Concurrent to Chien *et al.*'s observation, Anderson[8] proposed the clue to perceive the normal-state Hall anomaly by distinguishing between the relaxation rates for the carrier motion normal to the Fermi-surface and parallel to it. The theory especially predicts the behavior of the Hall angle when in-plane impurities are introduced. Consequently Chien *et al.* have confirmed this prediction by carrying out experiments on Zn-doped crystals of YBCO.

Thus, the current study on the normal-state resistivity and Hall effect in a series of YBCO/PBCO superlattices is expected to reveal valuable information regarding the transport properties of YBCO/PBCO superlattices. The present work aims to determine whether the charge density of the YBCO/PBCO superlattice is modified with variations in the layer thickness.

II. EXPERIMENT

Superconducting YBCO/PBCO superlattices were *in situ* grown onto a rotated $SrTiO_3(001)$ substrate in a rf magnetron sputtering system. A computer controlled the YBCO and PBCO sputtering guns and the shutters alternatively. YBCO and PBCO layers were alternatively deposited onto a $SrTiO_3(001)$ substrate until the desired thickness of a superlattice was reached. As is well known, a buffer PBCO layer improves the lattice matching between the MgO(001) substrate and the YBCO film.[9] A PBCO buffer layer 960 Å thick was hence grown onto the $SrTiO_3(001)$ substrate, prior to the growth of YBCO/PBCO superlattices. On top of the buffer, a stack consisting of n cells YBCO/m cells PBCO is deposited N times alternatively with the total thickness of YBCO layers $\approx$960 Å, where a unit-cell thickness $\approx$12 Å. The superlattice crystal structure was initially investigated by the x-ray diffraction. Figure 1 depicts the x-ray-diffraction spectra in the region near the (001) peak for the YBCO/PBCO (96 Å/60 Å), (96 Å/48 Å), and (60 Å/48Å) superlattices. In the θ-2θ x-ray scans for the samples on $SrTiO_3(001)$ only the $(00L)(L=1-7)$ diffraction peaks were observed, indicating a strong c-axis orientation. As Fig. 1 depicts, the satellite peaks on both sides of the main peak (001) confirm that a periodic structure in the superlattices has been achieved. The modulation wavelength, $D=D_1+D_2$, where D_1 and D_2 denote the thickness of the YBCO and PBCO layers, respectively, can be calculated from the separation of two successive peaks (i and $i+1$) using the equation $D=(\lambda/2)[1/(\sin\theta_i-\sin\theta_{i+1})]$, where λ represents the

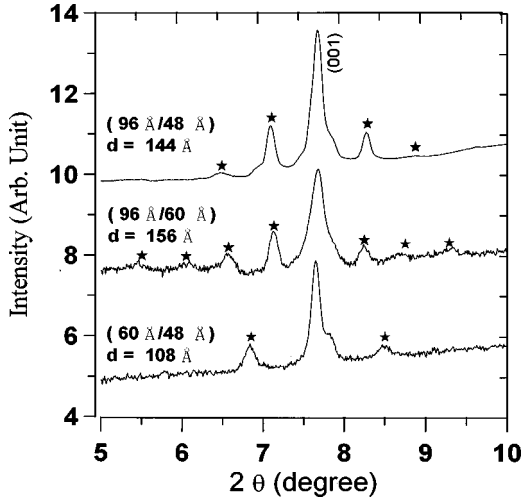

FIG. 1. θ-2θ x-ray-diffraction pattern of YBCO/PBCO (96 Å/60 Å), (96 Å/48 Å), and (60 Å/48 Å) superlattices. The satellite peaks are indicated by star symbols.

x-ray wavelength ($\lambda = 1.542$ Å). Thus, combining a precise calibration of deposition rate with x-ray-diffraction measurements, allows us to prepare a YBCO/PBCO superlattice with a desired thickness modulation. For the transport measurements, films were photolithographically patterned to a 2-mm-long by 100-μm-wide bridge containing two Hall terminals. Six gold dots were then evaporated onto the contact areas to allow simultaneous measurements of the resistive and Hall signals using standard dc techniques. Hall voltages were taken in oppose fields parallel to the c axis up to 5 T and at a dc current density of $J \sim 10^4$ A/cm^2.

III. RESULTS AND DISCUSSION

A. The resistivity and Hall number

Figures 2(a) and 2(b) depict the temperature dependence of the resistivity, ρ, and the Hall coefficient, R_H, for PBCO (1500-Å-thick) and YBCO (1500-Å-thick) thin films. The resistivity of PBCO film is $\sim 1 \times 10^{-2}$ Ω cm at 300 K and increases with a decreasing temperature. The Hall coefficient, R_H, remains positive and its magnitude increases monotonically with decreased temperature. The Hall coefficient of PBCO thin films exceeds that of YBCO thin films by a factor of about 100 at 300 K. All data are consistent with reported results.[10]

By using the formula $R = \rho(l/wd)$, we calculated the resistivity of superlattices with d equal to the total thickness of YBCO layers, where R is the resistance, l is the length, w is the width of the resistivity pattern. Figures 3(a) and 3(b) present $\rho(T)$ as a function of temperature for a series of YBCO/PBCO superlattices with various thickness of YBCO or PBCO layers. The resistivity of PBCO layers is much larger than that of YBCO layers, hence the transport current primarily flows along YBCO layers. The resistivity increases systematically in YBCO/PBCO superlattices with a fixed thickness of YBCO layers and increased thickness of PBCO [Fig. 3(a)]. On the other hand, the resistivity decreases in superlattices with a fixed thickness of PBCO layers and increased thickness of YBCO layers [Fig. 3(b)]. The inset of Fig. 3(a) shows the resistivity of a YBCO/PBCO (36 Å/60 Å) superlattice calculated by considering different film thickness. Curve B was calculated by the formula $R = \rho(l/wd)$, with d equal to the total thickness of YBCO layers while curve A was obtained with d equal to the total thickness of YBCO and PBCO layers. Notably, superlattices can be considered as independent resistors connected in parallel. The resistivity, ρ_{SL}, can be expressed as[11]

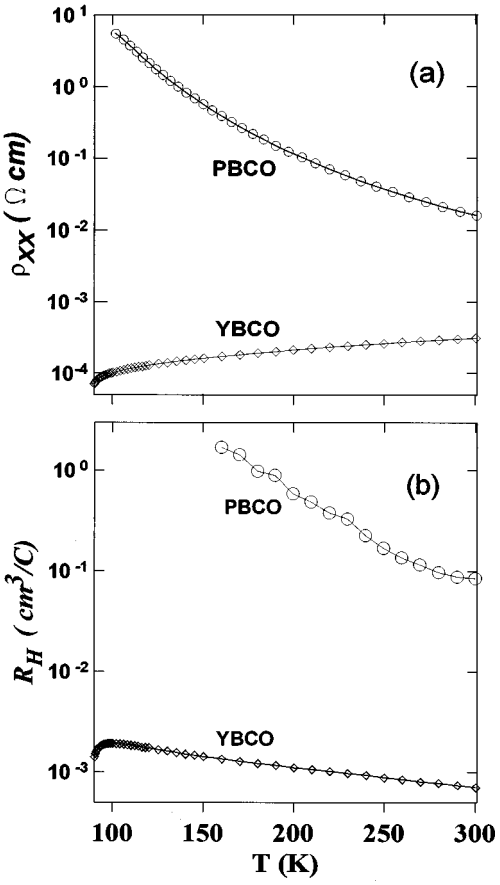

FIG. 2. (a) Resistivities as function of temperature for a PBCO film and a YBCO film. (b) The Hall coefficients as a function of temperature for a PBCO film and a YBCO film.

$$d/\rho_{\mathrm{SL}} = d_1/\rho_{\mathrm{YBCO}} + d_2/\rho_{\mathrm{PBCO}}, \tag{1}$$

where ρ_{YBCO} is the resistivity of YBCO layers, ρ_{PBCO} is the resistivity of PBCO layers, d_1 is the total thickness of YBCO layers, d_2 the total thickness of PBCO layers, and $d = d_1 + d_2$. The dashed line [YBCO/PBCO (36 Å/60 Å) superlattice] was obtained by Eq. (1) with d equal to the total thickness of YBCO and PBCO layers; while ρ_{YBCO} and ρ_{PBCO} are equal to the resistivity of YBCO and PBCO thin films. Curve B correlates well with Eq. (1) only if the total thickness of YBCO layers is considered. The results confirm that the transport current primarily flows along the YBCO layers in superlattices. A small discrepancy in the resistivity data is available because some scattering from the interfaces between YBCO layers and PBCO layers was not considered, tending to cause the measured resistivity to be higher than that of the calculated data for YBCO/PBCO (36 Å/60 Å) superlattice. Although the charge transfer between YBCO layers and PBCO layers[12,13] and other effects[14] presented a difficulty in estimating the resistivity, Hall coefficient, and

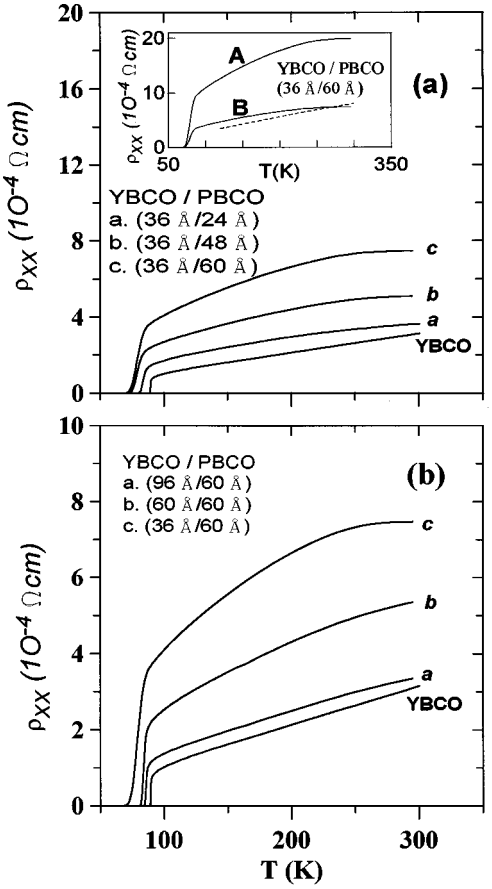

FIG. 3. Temperature dependence of the resistivity for a YBCO film and a series of YBCO/PBCO superlattices. The inset of (a) shows resistivity of a YBCO/PBCO (36 Å/60 Å) superlattice calculated with different total thickness. Curve *B* was calculated by the formula $R=\rho(l/wd)$, with d equals to the total thickness of YBCO layers while curve *A* was obtained from the same formula with d equal to the total thickness of YBCO and PBCO layers. R is the resistance, l is the length, w is the width, and d the thickness of the resistivity pattern.

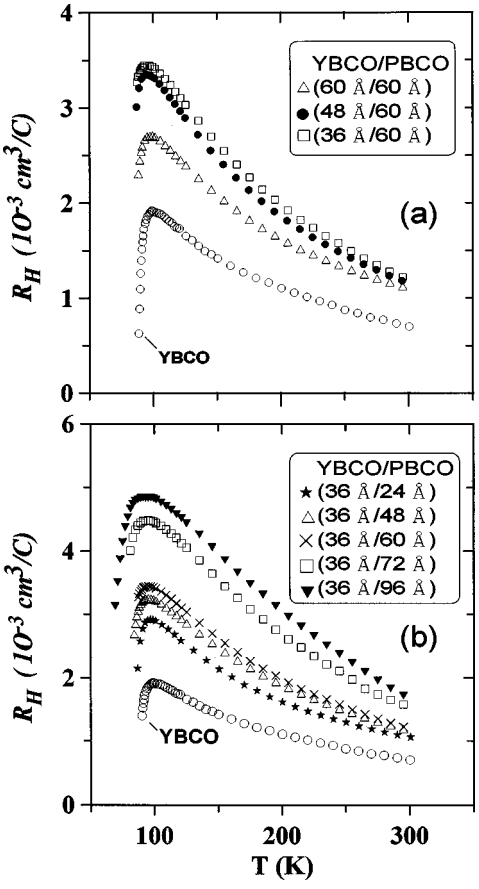

FIG. 4. Temperature dependence of Hall coefficient in a series of YBCO/PBCO superlattices: (a) $d_{\mathrm{YBCO}}=60$–36 Å with $d_{\mathrm{PBCO}}=60$ Å and (b) $d_{\mathrm{PBCO}}=24$–96 Å with $d_{\mathrm{YBCO}}=36$ Å.

Hall number quantitatively when the thickness of YBCO layers alone is considered; to the first-order approximation, the resistivity, Hall coefficient, and carrier concentration were assessed merely considering the total thickness of YBCO layers in the current work.

Table I displays the resistivity ρ, resistivity ratio $\rho(200\ \mathrm{K})/\rho(100\ \mathrm{K})$, Hall coefficient R_H, Hall number n_H, $T_c(50\%)$, and mean free path l, for a series of YBCO/PBCO superlattices. Those transport parameters were calculated by taking account of the total thickness of YBCO layers. The resistivities reveal a systematic change with variations in the layer thickness. The overall resistivity of the superlattices surpasses that of a YBCO (1650-Å-thick) thin film.

Figures 4(a) and 4(b) depict the Hall coefficient as a function of temperature for a series of YBCO/PBCO superlat-

TABLE I. Measured electronic parameters for various YBCO/PBCO superlattices and YBCO films. The values of resistivity, Hall coefficient and Hall number are calculated by taking only the thickness of YBCO layers.

Samples	ρ (200 K) ($\mu\Omega$ cm)	ρ (200 K) / ρ (100 K)	R_H (100 K) (10^{-3} cm^3/c)	R_H (200 K) (10^{-3} cm^3/c)	n_H (100 K) (1/cell)	n_H (200 K) (1/cell)	dn_H/dT (10^{-3}/cell K)	T_c (50%) (K)	l (100 K) (Å)
YBCO film	213.65	2.09	1.931	1.107	0.565	0.977	4.7±0.1	89.69	56.3
(96 Å/60 Å)	256.14	1.82	1.770	0.963	0.611	1.123	5.1±0.3	85.83	39.3
(60 Å/60 Å)	439.00	1.71	2.705	1.595	0.399	0.677	2.9±0.1	84.09	28.3
(48 Å/60 Å)	421.07	1.59	3.315	1.825	0.326	0.594	3.0±0.1	80.91	31.5
(36 Å/60 Å)	673.80	1.62	3.418	1.927	0.317	0.561	2.8±0.1	78.83	20.5
(36 Å/24 Å)	296.76	1.72	2.905	1.622	0.372	0.666	3.3±0.1	83.81	44.1
(36 Å/48 Å)	460.47	1.64	3.222	1.845	0.335	0.585	2.9±0.1	79.69	29.9
(36 Å/60 Å)	673.79	1.62	3.417	1.927	0.317	0.561	2.8±0.1	78.83	20.5
(36 Å/72 Å)	634.46	1.54	4.445	2.612	0.243	0.414	2.2±0.2	73.96	24.6
(36 Å/96 AA)	665.27	1.59	4.813	2.968	0.225	0.364	1.9±0.2	68.68	25.5

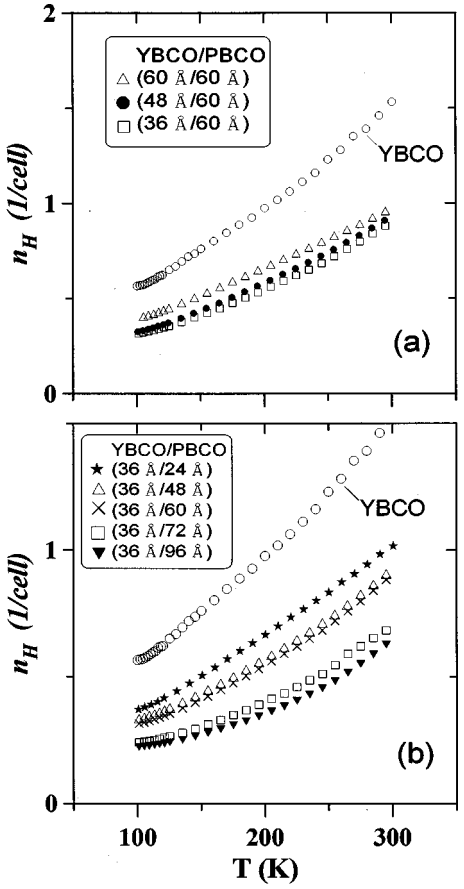

FIG. 5. Temperature dependence of Hall number in a series of superlattices: (a) $d_{\mathrm{YBCO}}=60$–36 Å with $d_{\mathrm{PBCO}}=60$ Å and (b) $d_{\mathrm{PBCO}}=24$–96 Å with $d_{\mathrm{YBCO}}=36$ Å.

tices, respectively, ($d_{\mathrm{YBCO}}=60$–36 Å/$d_{\mathrm{PBCO}}=60$ Å) and ($d_{\mathrm{YBCO}}=36$ Å/$d_{\mathrm{PBCO}}=24$–96 Å). These figures reveal that Hall coefficient R_H increases when the thickness of YBCO layers decreases. From Fig. 4(b), R_H increases as the thickness of PBCO layers is increased, i.e., R_H roughly depends on the ratio, $d_{\mathrm{YBCO}}/d_{\mathrm{PBCO}}$. The superconducting properties of $Y_{1-x}Pr_xBa_2Cu_3O_y$ has attracted considerable attention and experimentation[15–19] to perceive the role of rare-earth atom in high-T_c superconductors. Magnetic pair breaking, hole filling, or hole localization[15–19] are believed to be the major mechanism responsible for depressing the superconductivity. The mechanism for T_c depression, however, remains unclear for the YBCO/PBCO system. Systematic investigations of the Hall effect in $Y_{1-x}Pr_xBa_2Cu_3O_y$ alloys has been reported by Matsuda *et al.*[19] They have observed that R_H increases when Y is progressively substituted by Pr. These findings suggest that Pr is able to give rise to hole-filling effects in YBCO. Such a mechanism seems likely to be responsible for the observed increase in R_H in the present superlattices. Notably, a lower carrier density in the superlattices is consistent with higher resistivity data.

Figures 5(a) and 5(b) plot the variations in the Hall number $n_H(T)$ as a function of temperature and layer thickness. A systematic change in the Hall number with variation in the layer thickness can be observed. This observation apparently suggests the possibility of doping that may result rising from the substitution of PBCO layers for YBCO layers. However,

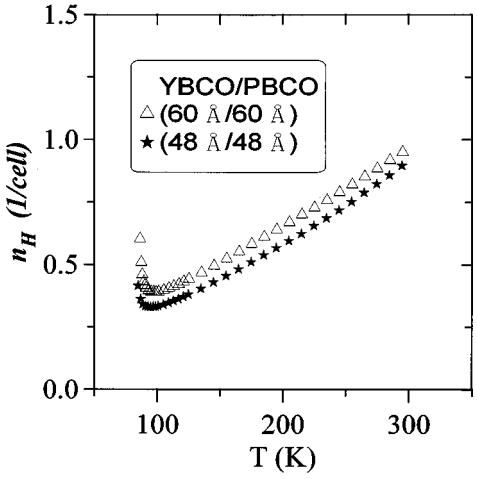

FIG. 6. Temperature dependence of Hall number for YBCO/PBCO (60 Å/60 Å) and (48 Å/48 Å) superlattices.

the current observation of the Hall effect in YBCO/PBCO superlattices cannot be expected to fully complement of the observations for $Y_{1-x}Pr_xBa_2Cu_3O_y$ alloys. This is evident from the difference in values of $n_H(T)$ curve can be observed for two superlattices samples: (60 Å/60 Å) and (48 Å/48 Å), both of which have the same $d_{\mathrm{YBCO}}/d_{\mathrm{PBCO}}$ ratio of 1:1 as shown in Fig. 6. Wood[13] reported theoretical study of the superconductivity in YBCO and PBCO alloys and layered films. He assessed the T_c suppression in both $Y_{1-x}Pr_xBa_2Cu_3O_y$ alloys as well as in YBCO/PBCO superlattices by a hole-filling mechanism with the charge transfer occurring near the interface, resulting in a variation in hole concentration in the superlattices. Our findings indicate that the critical temperature T_c for the superlattice is significantly higher than that in the corresponding $Y_{1-x}Pr_xBa_2Cu_3O_y$ alloys. Therefore the possibility of strong layer interdiffusion in our samples could be ruled out. This is also consistent with the presence of the satellite peaks as shown in the x-ray-diffraction spectra. Therefore, there is no reason to believe that the hole filling occurs over the superlattice periods. However, according to Wood's results, the charge transfer apparently occurs possibly near the interface only. Numerous investigations on the transport properties of the YBCO/PBCO superlattices are available. Several theoretical pictures have been proposed to explain the T_c depression in superlattices: (1) the proximity effect between the YBCO and PBCO layer,[20] (2) the hole-filling mechanism,[13] and the localization effect,[21] (3) the decoupling of the superconductors, which include the finite-size effect in layered superconductors[22] and the frustrated Josephson XY model,[23] etc. All these models introduce the T_c behavior and cause the common feature of the T_c variation in superlattices.

On the other hand, the linear temperature dependence of the Hall number in the superconducting oxides, as shown in Figs. 5(a) and 5(b), has not been completely perceived. Clayhold *et al.*[24] have observed that as the high-T_c behavior is suppressed, the unusual T dependence of n_H is also suppressed in the Co-doped and Ni-doped YBCO alloys. They also suggested that the strong T dependence of n_H could be intrinsic to the high-T_c oxides as well. Table I lists the slopes (dn_H/dT) of the n_H vs T curve, as obtained by linear fitting

between 100 and 220 K are also presented. dn_H/dT is lower for the superlattices with thinner YBCO layers or thicker PBCO layers.

B. The normal-state Hall angle

According to Anderson's theory,[8] the transverse (''Hall'') relaxation rate $1/\tau_H$ is determined by scattering between spin excitations, and varies as T^2. The scattering from magnetically active impurities introduces additional terms in the transport scattering rate, $1/\tau_{\rm tr}$ and Hall relaxation rate $1/\tau_H$. For the transverse scattering rate Anderson introduced

$$1/\tau_H = T^2/W_S + 1/\tau_M , \tag{2}$$

where W_S denotes the bandwidth of the spin excitations (the spin-exchange energy J in Anderson's theory) and $1/\tau_M$ is the impurity contribution. For the thin films of YBCO and YBCO/PBCO superlattices, the transport scattering rate $1/\tau_{\rm tr}$ is proportional to the resistivity, i.e., σ_{xx} which is in turn proportional to $\tau_{\rm tr}$, whereas σ_{xy} is proportional to $\tau_H\tau_{\rm tr}$. While, the Hall angle $\theta_H = \tan^{-1}(\sigma_{xy}/\sigma_{xx})$ involves $1/\tau_H$ only, Eq. (2) implies

$$\cot\theta_H = 1/\omega_c\tau_H = \alpha T^2 + C, \tag{3}$$

where $\omega_c = eB/m^*$, m^* being an effective mass and C the impurity contribution.

To verify Eq. (3), we plotted $\cot\theta_H$ vs T^2 for a series of YBCO/PBCO superlattices and a YBCO thin film in Figs. 7(a) and 7(b). For all samples investigated, the data points fall on a straight line in the temperature range below $\sim$220 K. Figures 7(a) and 7(b) depict $\cot\theta_H$ vs T^2 curves for YBCO/PBCO superlattices with a constant PBCO thickness of 60 Å [Fig. 7(a)] and a fixed constant YBCO thickness of 36 Å [Fig. 7(b)]. By using the line fitted to Eq. (3), we listed the parameters α and C in Table II. Table II lists the values of α that do not vary systematically with the variation in thickness of the YBCO or PBCO layer. However, the impurity contribution C tends to increase with an increasing $d_{\rm PBCO}$ or with a decreased $d_{\rm YBCO}$ value. Figure 8 plots the variations in the parameter C as a function of $d_{\rm YBCO}$ as well as $d_{\rm PBCO}$. The increase in the magnitude of the impurity contribution C corresponds to the observed enhancement of the resistivity for the present samples. This demonstrates that scattering by the PBCO layers decreases both τ_H and $\tau_{\rm tr}$.

Xiong *et al.*[25] reported on the temperature dependence of the Hall angle in oxygen-deficient and Pr-doped YBCO epitaxial films. They observed that in the $YBa_2Cu_3O_{7-y}$ system α increases monotonically with y, while the quantity C remains nearly constant. In the $Pr_xY_{1-x}Ba_2Cu_3O_7$ series both α and C increase with x. Thus, in conjunction with results obtained for other systems, Xiong *et al.* proposed that the behavior of $\cot\theta_H$ can be categorized into three groups: (1) α varies but C remains constant, as in $YBa_2Cu_3O_{7-y}$; (2) C varies but α remains constant, as observed for the Cu-site doped $YBa_2Cu_{1-x}A_xO_{7-y}$ system; and (3) both α and C vary, as typified by $Pr_xY_{1-x}Ba_2Cu_3O_{7-y}$. This categorization presents a unique approach to analyzing the Hall effect and offers a different way to understand the suppression of superconductivity in these systems. Thus, Xiang *et al.* concluded that the changes in α and C are attributed from two distinct mechanisms for suppressing superconductivity. While an increased C corresponds to a reduction in the carrier mobility, the variations in α reflect the variation in true carrier density.[25]

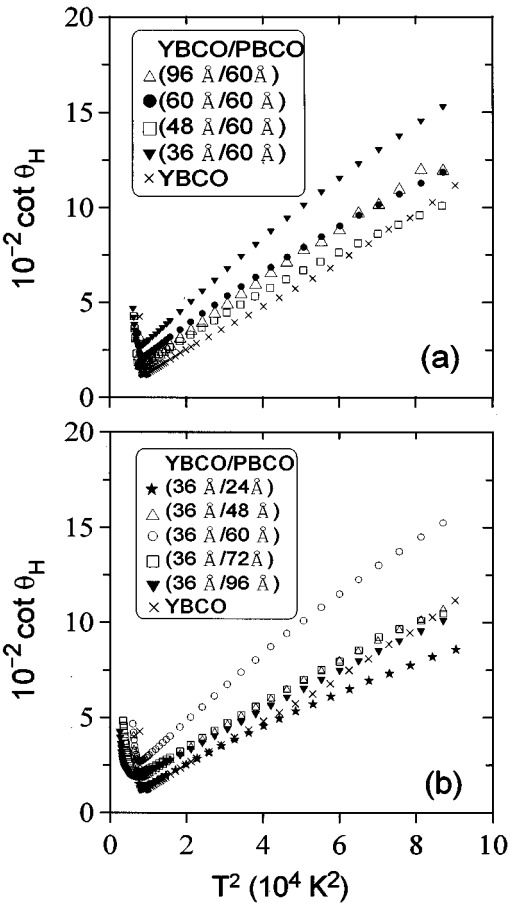

FIG. 7. Temperature dependence of the Hall angle shown as $\cot\theta_H$ vs T^2 for a series of YBCO/PBCO superlattices with (a) a constant PBCO thickness and (b) a constant YBCO thickness. $\cot\theta_H$ is computed from ρ_{xy} and ρ_{xx} measured on the sample.

In the YBCO/PBCO superlattices, the increased magnitude of C with an increase in $d_{\rm PBCO}$ indicates that the magnetic impurity introduced by PBCO layers couples with the

TABLE II. The parameters α and C deduced from the temperature dependence of Hall angle: $\cot\theta_H = \alpha T^2 + C$ for a series of YBCO/PBCO superlattices and a YBCO film.

Samples	$\alpha(\times 10^{-2}\ \mathrm{K}^{-2})$	C
(120 Å/60 Å)	1.029±0.020	72.44±12.24
(96 Å/60 Å)	1.374±0.039	78.48±17.55
(60 Å/60 Å)	1.404±0.022	100.72±10.08
(48 Å/60 Å)	1.079±0.026	108.09±11.88
(36 Å/60 Å)	1.830±0.016	116.70±7.20
(36 Å/24 Å)	0.903±0.026	77.25±11.70
(36 Å/48 Å)	1.144±0.022	109.41±10.17
(36 Å/60 Å)	1.830±0.016	116.70±7.20
(36 Å/72 Å)	1.110±0.024	125.53±10.35
(36 Å/96 Å)	1.017±0.017	129.54±6.84
(YBCO)	1.156±0.012	13.45±6.07

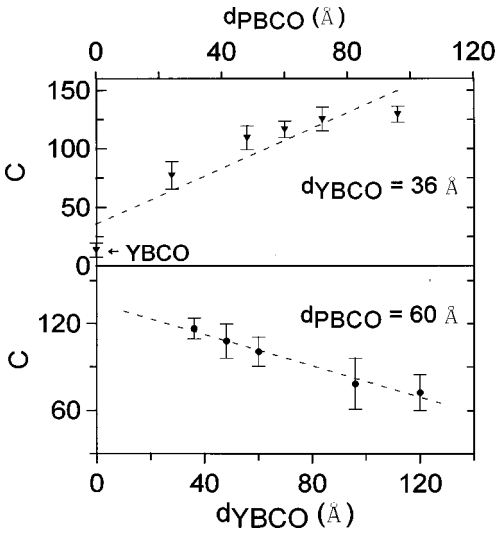

FIG. 8. Variations in impurity concentration C with variation in d_{PBCO} (upper panel) and d_{YBCO} (lower panel) in the same samples. The dashed lines are guides to the eye.

electronic states in the Cu-O_2 planes, as observed for Zn-doped YBCO single crystals.[7] The scattering of carriers by the Pr magnetic moments would then reduce the carrier mobility. If such a mechanism exists, the depression in T_c might possibly be caused by the magnetic scattering which induces the pair breaking. On the other hand, the slope α is suggested to be controlled by the carrier density and by the exchange parameter J as well. The slope α is the parameter most sensitive to carrier density. Nevertheless, this quantity of α, which varies but not systematically with variation in d_{YBCO} or d_{PBCO} in YBCO/PBCO superlattices, is not consistent with the variations in Hall number. Since both α and C vary in YBCO/PBCO superlattices, the hole-filling near the interface and pair breaking are likely to be the significant origins of the suppression of superconductivity in the YBCO/PBCO superlattice. The exact mechanism is, however, unclear owing to the insufficient resolution of α.

IV. CONCLUSION

In conclusion, we report that the average Hall coefficient R_H and Hall number n_H in YBCO/PBCO superlattices vary systematically with variations in the thickness in the individual YBCO or PBCO layers. $T_{c,\mathrm{zero}}$ decrease sharply from 90 K for YBCO films to 57 K for YBCO/PBCO (36 Å/96 Å) superlattice, corresponding to a higher resistivity and lower Hall number. The suppression of the Hall number in the YBCO/PBCO superlattices might result from the charge transfer occurring near the interface only. Additionally, the Hall angle follows $\cot\theta_H=\alpha T^2+C$ in all YBCO/PBCO superlattices, where both α and C vary with variations in YBCO and PBCO thickness. The simultaneous variations in α and C with different layer thicknesses in YBCO/PBCO superlattices suggest that the reduction in carrier density, attributed to the magnetic scattering and charge transfer which occur near the interface, leads to the depression of T_c in the YBCO/PBCO superlattice.

ACKNOWLEDGMENTS

The authors would like to thank National Science Council of Republic of China for financial support under Contract Nos. NSC85-2112-M002-027PH, NSC86-2112-M003-013, and NSC86-2112-M002-033.

[1] J. M. Triscone, M. G. Karkut, L. Antogazza, O. Brunner, and Ø. Fischer, Phys. Rev. Lett. **63**, 1016 (1989).
[2] X. D. Wu, X. X. Xi, Q. Li, A. Inam, B. Dutta, L. DiDomenico, and C. Weiss, Appl. Phys. Lett. **56**, 400 (1990).
[3] A. Gupta, R. Gross, E. Olsson, A. Segmciller, G. Koren, and C. C. Tsuei, Phys. Rev. Lett. **64**, 3191 (1990).
[4] J. M. Triscone, Ø. Fischer, O. Brunner, L. Antognazza, A. D. Kent, and M. G. Karkut, Phys. Rev. Lett. **64**, 804 (1990).
[5] D. H. Lowndes, D. P. Norton, and J. D. Budai, Phys. Rev. Lett. **65**, 1160 (1990).
[6] M. Affronte, J.-M. Triscone, O. Brunner, L. Antognazza, L. Miéville, M. Decroux, and Ø. Fischer, Phys. Rev. B **43**, 11 484 (1991).
[7] T. R. Chien, Z. Z. Wang, and N. P. Ong, Phys. Rev. Lett. **67**, 2088 (1991).
[8] P. W. Anderson, Phys. Rev. Lett. **67**, 2092 (1991).
[9] L. M. Wang, H. H. Sung, J. H. Chern, H. C. Yang, and H. E. Horng, Chin. J. Phys. **31**, 1031 (1993).
[10] Y. X. Jia, J. Z. Liu, A. Matsushita, M. D. Lan, P. Klavins, and R. N. Shelton, Phys. Rev. B **46**, 11 745 (1992).
[11] D. K. C. MacDonald, *Thermoelectricity: An Introduction to the Principles* (Wiley, New York, 1962).
[12] J. Z. Wu, C. S. Ting, W. K. Chu, and X. X. Yao, Phys. Rev. B **44**, 411 (1991).
[13] R. F. Wood, Phys. Rev. Lett. **46**, 829 (1991).
[14] G. Liu, G. Xiong, G. Li, G. Lian, K. Wu, S. Liu, J. Li, and S. Yan, Phys. Rev. B **49**, 15 287 (1994).
[15] A. P. Goncalves, I. C. Santos, E. B. Lopes, R. T. Henriques, M. Almeida, and M. O. Figueriedo, Phys. Rev. B **37**, 7476 (1988).
[16] A. D. Kent, J. M. Triscone, L. Antognazza, O. Brunner, C. Renner, P. Niedermann, M. G. Karkut, and Ø. Fischer, Physica B **165&166**, 1503 (1990).
[17] N. E. Phillips, R. H. Fisher, R. Gaspary, and A. Amuto, Phys. Rev. B **43**, 1148 (1991).
[18] G. Hilscher, E. Holland-Moritz, T. Holubar, H.-D. Jostarndt, V. Nekvasil, G. Schaudy, U. Walter, and G. Fillion, Phys. Rev. B **49**, 535 (1994).
[19] A. Matsuda, K. Kinoshita, T. Ishii, H. Shibata, F. Watanabe, and T. Yamada, Phys. Rev. B **38**, 2910 (1988).
[20] N. Zou and L. Hu, J. Low Temp. Phys. **80**, 69 (1990).
[21] S. Maekawa and H. Fukuyama, J. Phys. Soc. Jpn. **51**, 1380 (1981).
[22] K. Michielsen, T. Schneider, and H. De Raedt, Z. Phys. B **85**, 15 (1991).
[23] B. A. Cherenkov, Sov. Phys. Solid State **34**, 1437 (1992).
[24] J. Clayhold, N. P. Ong, Z. Z. Wang, J. M. Tarascon, and P. Barboux, Phys. Rev. B **39**, 7324 (1989).
[25] P. Xiong, G. Xiao, and X. D. Wu, Phys. Rev. B **47**, 5516 (1993).